# High Thermal Conductivity of a Hydrogenated Amorphous Silicon Film

Xiao Liu,[1] J. L. Feldman,[1,2] D. G. Cahill,[3] R. S. Crandall,[4] N. Bernstein,[1] D. M. Photiadis,[1] M. J. Mehl,[1] and D. A. Papaconstantopoulos[1,2]

[1]*Naval Research Laboratory, Washington, D.C. 20375, USA*

[2]*Department of Computation and Data Sciences, George Mason University, Fairfax, Virginia 22030, USA*

[3]*Frederick Seitz Materials Research Laboratory and Department of Materials Science and Engineering, University of Illinois, Urbana, Illinois 61801, USA*

[4]*National Renewable Energy Laboratory, Golden, Colorado 80401, USA*

(Received 18 September 2008; published 21 January 2009)

We measured the thermal conductivity $\kappa$ of an 80 $\mu$m thick hydrogenated amorphous silicon film prepared by hot-wire chemical-vapor deposition with the $3\omega$ (80–300 K) and the time-domain thermoreflectance (300 K) methods. The $\kappa$ is higher than any of the previous temperature dependent measurements and shows a strong phonon mean free path dependence. We also applied a Kubo based theory using a tight-binding method on three 1000 atom continuous random network models. The theory gives higher $\kappa$ for more ordered models, but not high enough to explain our results, even after extrapolating to lower frequencies with a Boltzmann approach. Our results show that this material is more ordered than any amorphous silicon previously studied.

DOI: 10.1103/PhysRevLett.102.035901 PACS numbers: 65.60.+a, 61.43.Dq, 63.50.−x, 66.70.−f

One of the long standing issues in solid state physics is the nature of thermal conduction in glasses and amorphous semiconductors. A preponderance of research efforts have been devoted to low temperatures, where the $T^2$ dependent thermal conductivity $\kappa$ below 1 K is thought to result from phonon scattering by atomic tunneling states (TS), common in amorphous solids but unknown in origin [1]. The physical mechanisms that lead to the universal features in bulk amorphous materials such as the plateau near 10 K [2–5], the further rise of $\kappa$ above 40 K, and the near saturation at higher $T$ are still debated [2–8]. The 100 year old Einstein theory [9], the minimum thermal conductivity concept [6,7], the fracton theory [3], and a Kubo based theory [8] have all been applied to the high temperature regime. The minimum thermal conductivity concept provides an explanation of $\kappa(T)$ above the plateau in a phenomenological way in terms of an assumed phonon mean free path $\ell$ either on the order of the phonon wavelength or the lattice spacing. In contrast, the fracton theory asserts that anharmonicity induced hopping transport between localized phonon modes accounts for $\kappa$ in this same temperature range. The Kubo based theory uses a specific continuous random network (CRN) structure model and a realistic interatomic potential to compute the phonon spectrum. It has provided a description of $\kappa$ for amorphous silicon ($a$-Si) [10–12] in reasonable agreement with experiment.

In this Letter, we report on temperature and laser-modulation-frequency dependent measurements of $\kappa$ of an 80 $\mu$m thick hydrogenated $a$-Si ($a$-Si:H) film with 1 at. % H prepared by hot-wire chemical-vapor deposition (HWCVD). This novel $a$-Si:H, emergent as a new material for technological applications [13], has higher medium range order, higher mass density, less defect density, and lower residual stress than other $a$-Si:H [13]. It also has a surprisingly different hydrogen distribution from other $a$-Si:H [14]. In particular, the internal friction is more than 2 orders of magnitude lower than any other amorphous solids below 10 K, a result which has been explained by the almost complete lack of TS [15]. In this work, we show that its $\kappa$ has the typical $T$ dependence of a glass but is at least about a factor of 2 higher than previous $T$ dependent measurements on $a$-Si(:H), aside from one [16] that has largely been ignored [17] in the literature. We also show a strong phonon mean free path dependence with $\ell$ up to 612 nm still contributing to $\kappa$, in conflict with the minimum thermal conductivity concept. To explain the results, we have performed improved Kubo based calculations using a tight-binding (TB) electronic structure method and examined three different CRN based models of $a$-Si [18]. We find that the theory gives higher $\kappa$ for more structurally ordered models within the wavelength limit of their finite size, but not high enough to explain our results, even after extrapolating to lower frequencies with a Boltzmann approach, a result which we take as evidence that our sample is more ordered than the simulation structures, and further, more ordered than a typical $a$-Si(:H).

The $a$-Si:H film was deposited on a stainless steel substrate at 430 °C for 8 h. Its surface was polished to remove hydrogen bubbles. Although a similarly prepared 2 $\mu$m thick film was characterized previously to be fully amorphous by high resolution TEM and electron diffraction [15], Raman measurement on this film again showed its spectrum was the same as a typical $a$-Si. The standard $3\omega$ method [19] was used to measure $\kappa$ from 80–300 K. The time-domain thermoreflectance (TDTR) experiments [20] were performed to probe the phonon mean free path dependence of $\kappa$ at 300 K by varying the pulsed-laser modulation frequencies.

 

The results of the $3\omega$ measurements are shown in Fig. 1 together with most of the $T$ dependent results published so far. Figure 1(a) focuses on measurements above 40 K, while Fig. 1(b) shows four more measurements that extend to below 10 K. We note that $a$-Si(:H) can have different microstructures depending on film preparation, hydrogenation, and heat treatment that may all impact $\kappa$. If boundary scattering dominates, $\kappa$ could also show a film thickness dependence. The variation of $\kappa$ in $a$-Si(:H) may have been further complicated by the difficulties for measuring $\kappa$ of thin films. While most of the $\kappa(T)$ in Fig. 1 show values between 1 and 2.5 W/mK near 300 K [11,12,19,21], room temperature only measurements show a wider variation, to as high as 4–6 W/mK in a few indirect measurements based on diffusivity [22] (not shown). At 300 K, our result is almost the same as the thermally evaporated $a$-Si [16]. Over the entire temperature range covered, our result is significantly larger than any of the previous ones. In those previous measurements, no systematic dependence on H content, varying from 1 to 20 at. %, was found on sputtered $a$-Si:H films [11] (for clarity, only 1 and 15 at. % results are shown). Below 50 K, a plateau was observed on sputtered $a$-Si [21], and a roughly linear $T$ dependence was observed on the thermally evaporated [16] and $e$-beam evaporated [12] $a$-Si.

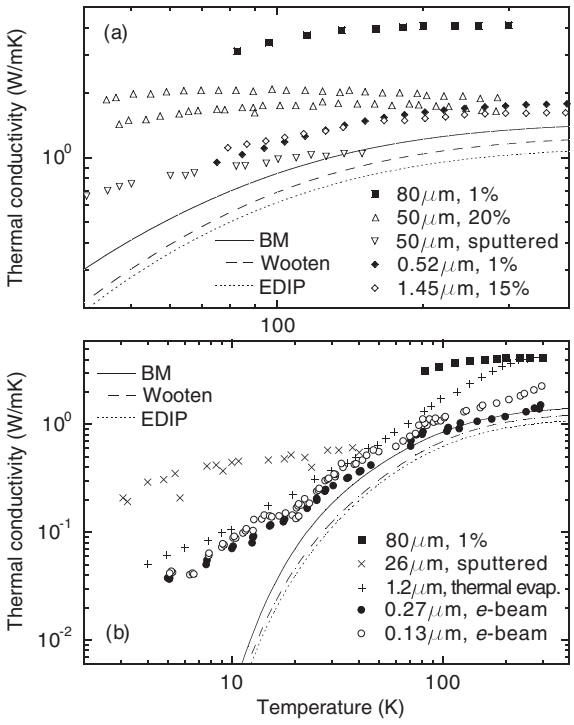


FIG. 1. $\kappa$ of $a$-Si(:H) vs $T$. Our $3\omega$ results are compared with previous ones: (a) above 40 K, (b) down to 2 K. The 80 $\mu$m data are from this work; the 50 $\mu$m, Ref. [19]; the 26 $\mu$m, Ref. [21]; the 0.52 and 1.45 $\mu$m, Ref. [11]; the 1.2 $\mu$m, Ref. [16]; the 0.13 and 0.27 $\mu$m, Ref. [12]. The Kubo based theory results for the three CRN models as detailed later in the text are represented by the lines labeled.

The TDTR measurements show $\kappa$ to be 4.5, 3.9, and 2.8 W/mK at 300 K for modulation frequencies of the pump beam of 1.11, 3.35, and 9.8 MHz, respectively. In the limit of low modulation frequency, our $3\omega$ and TDTR results agree within 10%. In a TDTR experiment, phonons with $\ell$ longer than the spatial extent of the $T$ gradient do not contribute to the measured value of $\kappa$ [20]. The agreement between the $3\omega$ and the TDTR measurements at 1.11 MHz suggests that phonons with $\ell > (D/\omega)^{1/2} = 612$ nm are not significant for thermal conduction in this sample. Furthermore, the difference between the high and low frequency measurements by TDTR indicates that phonons with $162 < \ell < 612$ nm contribute ~40% of the $\kappa$ of the sample.

We apply Kubo based theory in the harmonic approximation to compute the vibrational spectrum using a TB electronic structure total energy method [23] with the parameters derived from Ref. [24]. Anharmonicity has been shown to have a small effect on $\kappa$ [25]. We use three 1000 atom CRNs which differ in structural ordering (see Ref. [18] and references therein) and are all ''relaxed'' within our TB method. The Wooten model is based on an initial diamond structure and a bond switching algorithm, the Barkema and Mousseau (BM) model uses a generated random distribution as an initial configuration, and the environment dependent interatomic potential (EDIP) model is based entirely on a molecular dynamics quench from the liquid. The Kubo based theory has been applied to the same 1000 atom Wooten model with the Stillinger-Weber potential (SWP) [10].

Comparisons of the vibrational densities of states with inelastic neutron scattering [26] are shown in Fig. 2 for all three CRNs, which reveals very little difference among models and remarkable agreement with experiment for the peak centered at 20 meV. The disagreements seen at higher energies are well outside experimental uncertainty. Since TB method also yields frequencies slightly higher than those of the crystal [24], the disagreement with experiment may be safely associated with our theory rather than with the models. Although similar high-frequency discrepancies result for the SWP, the TB method represents a significant improvement over the SWP for the vibrational spectrum at low frequencies [27].

The acoustic projected spectral density $S(Q, E)$ is shown in Fig. 3. From the $\mathbf{Q} = \langle 100 \rangle$ transverse and longitudinal projections, we obtain the respective phase velocities of $v_t = 4.74 \times 10^5$ and $v_l = 7.83 \times 10^5$ cm/s for the Wooten model. Slightly higher and lower values are obtained for the BM and EDIP models, respectively. The above $v_t$ is within a few percent of the experimental sound velocities of ion-implantation amorphized silicon [28]. Sound velocities for HWCVD $a$-Si:H films are still unknown, but this material has a mass density close to that of ion-implantation amorphized Si [29]. Unlike the vibrational densities of states, our results also show that different CRN models can produce substantially different

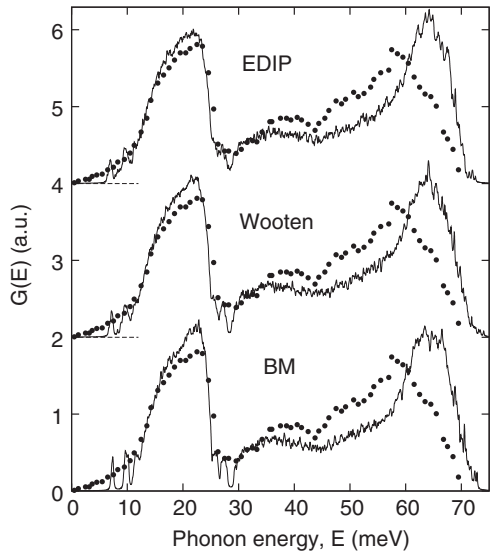


FIG. 2. Comparison of calculated vibrational density of states for the three CRNs with the results of inelastic neutron scattering (●) [26].

spectral density properties at low frequencies. Not surprisingly, we find that for the three CRNs compared in Fig. 3 the peak sharpness increases with increasing structural order. For example, the BM model, which has the sharpest peaks, also has the lowest energy structure [18].

The Kubo based theory expresses $\kappa_{\mathrm{Kubo}}$ as an autocorrelation function of an energy current operator $S$. In practice, due to discreteness in normal mode frequencies as a result of finite size of the models, the theory relies on an extrapolation of an applied frequency ($\Omega$) dependent $\kappa$ to $\Omega = 0$. Finite $\kappa$ at small $\Omega$ comes from a nonzero overlap quantity, $\langle i|S_x|j\rangle$, involving the dynamical matrix, equilibrium positions, and pairs of normal mode eigenvectors $|i\rangle$

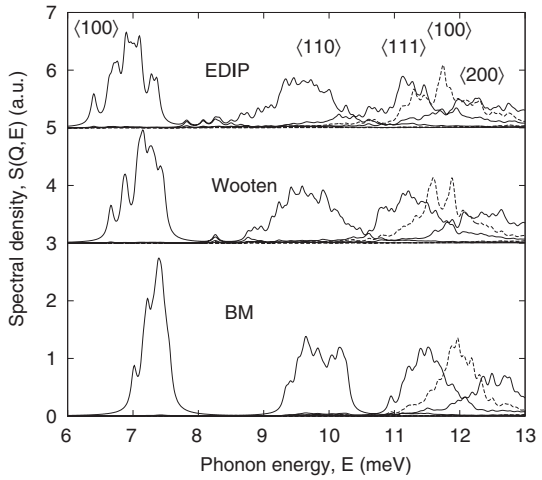


FIG. 3. $S(Q, E)$ for eigenvectors projected onto transverse (solid line) and longitudinal (dashed line) directions for the three CRNs. Sets of $\mathbf{Q}$ corresponding to each peak are indicated in units of $2\pi/L$, where $L = 27.26$ Å is the length of the computational cell.

of nearby frequencies [8,10]. $\kappa_{\mathrm{Kubo}}$ can be written as

$$\kappa_{xx}(\Omega, T) = \frac{\pi}{VT}\sum_{i,j}\frac{n_j - n_i}{\hbar\omega_{ij}}|\langle i|S_x|j\rangle|^2\delta_\eta(\omega_{ij} - \Omega), \quad (1)$$

where $n_i$ represents the Bose occupation, $\omega_{ij}$ is a normal mode frequency difference $\omega_i - \omega_j$, and $\delta_\eta$ is a Lorentzian of broadening parameter $\eta$ [8,10]. The numerical results given here average $\kappa_{ii}$ for $i = x, y, z$.

Figure 4 shows an example of obtaining $\kappa_{\mathrm{Kubo}}$ at 300 K for the BM model, where the effect of $\eta$ and the extrapolating process are demonstrated. We choose $\eta = 0.022$ meV for all three models labeled in Fig. 1. Although we see a clear dependence of $\kappa_{\mathrm{Kubo}}$ on the structural ordering of the models in Fig. 1, the values of $\kappa_{\mathrm{Kubo}}$ are smaller than any of the experimental results, even smaller than that of the TDTR at 9.8 MHz. Similar results have been interpreted in the past as due to contributions from low frequency modes omitted from finite size of the models. It is necessary to augment the total $\kappa$ with low frequency contributions $\kappa_{\mathrm{L}}$, i.e., $\kappa = \kappa_{\mathrm{Kubo}} + \kappa_{\mathrm{L}}$. We consider approaches adopted by Cahill *et al.* [11] for thin films and by Feldman *et al.* [10] for thicker films, where boundary and TS scattering, respectively, were assumed to play a significant role. We then employed a quartic, i.e., Rayleigh, phonon scattering rate that was fit at the lower frequency limit of the computational model to the mode diffusivity, and used a Boltzmann transport theory that includes boundary scattering [30] and anharmonic scattering (estimated from numerical studies on crystalline silicon [31]). No TS scattering was included in this estimate because of the above-mentioned characteristics of the sample. With this model, which admittedly is most appropriate for a lateral steady state measurement, we can obtain $\kappa$ as high as our experimental results. However, we have to include significant contributions from phonons with $\ell$ of the order of the sample thickness, incompatible with the nature of the $3\omega$ method and, more dramatically, with our TDTR measurements, which indicate $\ell \leq 612$ nm. The only physical model that we are aware of that yields larger $\kappa$, yet still

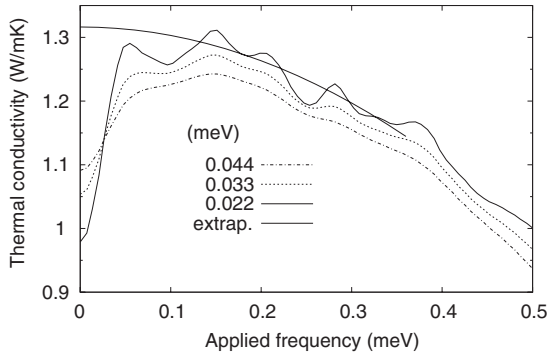


FIG. 4. The dependence of $\kappa_{\mathrm{Kubo}}$ for the BM model on an applied frequency $\Omega$ and the broadening parameter $\eta$ at 300 K is shown. The quadratic fit (over 0.12–0.36 meV) is used to extrapolate to $\Omega = 0$.

an amorphouslike $T$ dependence, is a nanocrystalline model [32], which is not applicable here. Instead, many experiments show that a judicious incorporation of a small amount H is the key for the superior material properties of this HWCVD sample [14,15]. Therefore, a well ordered $a$-Si:H model that incorporates the right amount of H [33], or even a paracrystalline $a$-Si:H model [34], may be needed to achieve a better description of our results.

Our results may also shed light on the nature of phonon attenuation in disordered materials, a subject which is still not well understood [35,36]. The sound attenuation due to disorder at low frequencies is thought to vary as $\omega^4$, while the attenuation due to disorder at higher frequencies ($Q \geq 1\ \mathrm{nm}^{-1}$) has been observed to vary as $\omega^2$. If we assume that the three TDTR data points correspond to the $\kappa$ from phonons with $\ell$ less than the spatial extent of the thermal gradients, i.e., 162, 328, and 612 nm, we can extract a simple scattering law as well as the phonon frequencies associated with these $\ell$ values. We find that a scattering rate of $\omega^2$ best represents the relative differences in $\kappa$ between the points, and the model leads to the TA phonon frequencies 5.94, 4.18, and 3.06 meV (wave numbers 1.90, 1.34, 0.98 $\mathrm{nm}^{-1}$); this $\omega^2$ behavior is consistent with previous results in this wave number domain [35]. However, the same scattering law extended to zero frequency would lead to an additional $\kappa$ of $\sim$1.7 W/mK with $\ell > 612$ nm, a prediction which is not borne out by our measurements. Further, the $\ell$ is expected to increase at a greater rate associated with Rayleigh scattering at lower frequencies [35], leading to an even larger contribution. The scattering mechanism responsible for the abrupt cutoff and strong suppression of the low frequency phonons is unknown.

We conclude that the high value of $\kappa$ and strong phonon mean free path dependence of the HWCVD $a$-Si:H discovered in this work points to an amorphous structure that differs in a significant way from other $a$-Si(:H) where the Kubo based theory seems to work well. This is consistent with the many other novel properties this amorphous material has manifested in prior studies, results which indicate that the HWCVD $a$-Si:H is much more ordered than other $a$-Si(:H).

We thank Dr. B. P. Nelson for preparing the 80 $\mu$m sample used in this work. We also thank Dr. P. B. Allen, Dr. R. O. Pohl, and Dr. S. Nakhmanson for helpful conversations. This work is supported by the Office of Naval Research.

[1] R. O. Pohl, X. Liu, and E. Thompson, Rev. Mod. Phys. **74**, 991 (2002).
[2] J. J. Freeman and A. C. Anderson, Phys. Rev. B **34**, 5684 (1986).
[3] S. Alexander, O. Entin-Wohlman, and R. Orbach, Phys. Rev. B **34**, 2726 (1986).
[4] P. B. Allen *et al.*, Philos. Mag. B **79**, 1715 (1999).
[5] V. Lubchenko and P. G. Wolynes, Proc. Natl. Acad. Sci. U.S.A. **100**, 1515 (2003).
[6] G. A. Slack, in *Solid State Physics: Advances in Research and Applications*, edited by H. Ehrenreich *et al.* (Academic, New York, 1979), Vol. 34, p. 1.
[7] D. G. Cahill and R. O. Pohl, Annu. Rev. Phys. Chem. **39**, 93 (1988).
[8] P. B. Allen and J. L. Feldman, Phys. Rev. Lett. **62**, 645 (1989); Phys. Rev. B **48**, 12 581 (1993).
[9] A. Einstein, Ann. Phys. (Leipzig) **35**, 679 (1911).
[10] J. L. Feldman *et al.*, Phys. Rev. B **48**, 12 589 (1993).
[11] D. G. Cahill, M. Katiyar, and J. R. Abelson, Phys. Rev. B **50**, 6077 (1994).
[12] B. L. Zink, R. Pietri, and F. Hellman, Phys. Rev. Lett. **96**, 055902 (2006).
[13] A. H. Mahan, Solar Energy Mater. Sol. Cells **78**, 299 (2003).
[14] Y. Wu *et al.*, Phys. Rev. Lett. **77**, 2049 (1996).
[15] X. Liu *et al.*, Phys. Rev. Lett. **78**, 4418 (1997); X. Liu and R. O. Pohl, Phys. Rev. B **58**, 9067 (1998).
[16] L. Wieczorek, H. J. Goldsmid, and G. L. Paul, in *Thermal Conductivity 20*, edited by D. P. H. Hasselman and J. R. Thomas (Plenum, New York, 1989), p. 235.
[17] This, and some other experiments on the thermal conductivity of $a$-Si(:H) mentioned later, inexplicitly assumed no effects of interfacial scattering. They have not yet been validated on samples with known thermal conductivity.
[18] J. L. Feldman *et al.*, J. Phys. Condens. Matter **16**, S5165 (2004).
[19] D. G. Cahill *et al.*, J. Vac. Sci. Technol. A **7**, 1259 (1989).
[20] Y. K. Koh and D. G. Cahill, Phys. Rev. B **76**, 075207 (2007).
[21] G. Pompe and E. Hegenbarth, Phys. Status Solidi B **147**, 103 (1988).
[22] B. S. W. Kuo, J. C. M. Li, and A. W. Schmid, Appl. Phys. A **55**, 289 (1992); L. Wei *et al.*, J. Mater. Res. **10**, 1889 (1995).
[23] R. E. Cohen, M. J. Mehl, and D. A. Papaconstantopoulos, Phys. Rev. B **50**, 14 694 (1994); M. J. Mehl and D. A. Papaconstantopoulos, *ibid.* **54**, 4519 (1996).
[24] N. Bernstein *et al.*, Phys. Rev. B **62**, 4477 (2000); **65**, 249902 (2002).
[25] Y. H. Lee *et al.*, Phys. Rev. B **43**, 6573 (1991).
[26] W. A. Kamitakahara *et al.*, Phys. Rev. B **36**, 6539 (1987).
[27] J. L. Feldman *et al.*, Phys. Rev. B **70**, 165201 (2004); **73**, 169905 (2006).
[28] R. Vacher, H. Sussner, and M. Schmidt, Solid State Commun. **34**, 279 (1980); X. Zhang *et al.*, Phys. Rev. B **58**, 13 677 (1998); S. I. Tan, B. S. Berry, and B. L. Crowder, Appl. Phys. Lett. **20**, 88 (1972).
[29] Z. Remes *et al.*, Phys. Rev. B **56**, R12 710 (1997).
[30] E. Ziambaras and P. Hyldgaard, J. Appl. Phys. **99**, 054303 (2006).
[31] A. Balandin and K. L. Wang, Phys. Rev. B **58**, 1544 (1998).
[32] A. Bodapati *et al.*, Phys. Rev. B **74**, 245207 (2006).
[33] P. Biswas, R. Atta-Fynn, and D. A. Drabold, Phys. Rev. B **76**, 125210 (2007).
[34] P. M. Voyles *et al.*, Appl. Phys. **90**, 4437 (2001).
[35] C. Masciovecchio *et al.*, Phys. Rev. Lett. **97**, 035501 (2006).
[36] G. Baldi *et al.*, Europhys. Lett. **78**, 36 001 (2007).